
# AN EXPERIMENTAL INVESTIGATION OF TURBULENT BOUNDARY-LAYER INTERACTION WITH DIFFERENT SERRATED TRAILING-EDGE CONFIGURATIONS

Aravind Sivakumar[1], Ric Porteous[1], Akhilesh Mimani[1] and Con J. Doolan[2]

[1]School of Mechanical Engineering
University of Adelaide, SA 5005, Australia
Email: aravind.sivakumar@student.adelaide.edu.au
ric.porteous@adelaide.edu.au
akhilesh.mimani@adelaide.edu.au

[2]School of Mechanical and Manufacturing Engineering
UNSW Australia, Sydney NSW 2052, Australia
Email: c.doolan@unsw.edu.au

## Abstract

The paper presents an experimental investigation of a turbulent boundary-layer interaction over a single large triangular serration at the Trailing-Edge (TE) of an airfoil on the flow-induced noise. Experiments were conducted at low-to-moderate Reynolds number given by $1.8 \times 10^5 < \mathrm{Re}_c < 5.7 \times 10^5$, where $c$ is the chord of airfoil. Six different TE serration geometries were studied: Three serrations with a single large triangular geometry at the TE, two serrations with varying orientation relative to the airfoil, and a straight-edged reference plate (in which the TE triangular serration is not considered). The airfoils with different TE configurations were placed in an anechoic wind tunnel in a mean flow field with free-stream velocities of 25, 30 and 35 $\mathrm{m \cdot s^{-1}}$. The radiated acoustic pressure field was recorded using a spiral microphone array located in the far-field. It was found that a significant noise reduction up to 6 dB was obtained when the included angle of the triangular serration was less than $45^\circ$, which was in agreement with Howe's theory. The Conventional Beamforming (CB) source maps confirmed that the noise reduction was obtained by varying the included angle of the triangular serrations. It was observed that the maximum noise attenuation occurred at frequencies above 5 kHz, where the TE noise dominates over the Leading-Edge (LE) noise. For frequencies below 5 kHz, the LE noise sources dominate over the TE noise.

## 1. Introduction

A steady uniform flow over an airfoil produces noise, predominantly located near the Trailing-Edge (TE) at a high-frequency range. In most real world applications, the main cause of the production of the TE noise is turbulent flow interacting with sudden impedance change of the edge [1]. Howe [2] showed that TE noise attenuation could be achieved by reducing the span-wise length of the TE. The effective reduction in TE noise is characterised by the wavenumber vector $\vec{\mathbf{K}}$ along the plane of the airfoil [2]. Chase [3] showed a relation between the wave vector and the spectral density of the hydrodynamic pressure field $P\left(\vec{\mathbf{K}},\omega\right)$ to the noise radiated from the TE in low Mach number turbulent flows. Later, it was shown that when the turbulent eddy structures convect over the TE with a free-stream velocity $U_\infty$, a tonal sound of angular frequency $\omega = U_\infty \times \vec{\mathbf{K}}_1$ is generated [3]. It is noted that

$\vec{\mathbf{K}}_1$ is the component of wavenumber vector, normal to the mean flow direction. The wavenumber vector $\vec{\mathbf{K}}_1$ provides information on the TE noise sources. The expected noise reduction is in high-frequency regions between the Strouhal number ($St_t$) range of 0.08 to 0.18. The principal acoustic sources are found only at the elements of TE that are inclined at an included half-angle $\vartheta$ greater than $45^o$ to the direction of air flow [2]. Hence, the analytical observations [2] suggested that a substantial reduction in the TE noise levels can be achieved, when the TE serrations are inclined at an included half-angle $\vartheta$ less than $45^o$ to the mean flow direction. Figures 1(a) and (b) show the angle of orientation of the edge with respect to the mean flow direction.

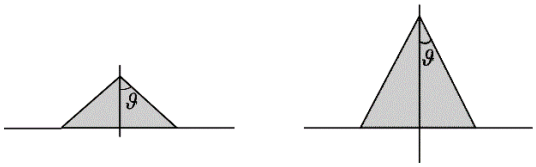


Figure 1. (a) Edge half-angle $\vartheta$ greater than $45^o$ to the mean flow direction and (b) Edge half-angle $\vartheta$ less than $45^o$ to the mean flow direction.

A previous experimental study has shown that both narrow and wide serrations at the TE reduce the flow-induced noise by suppressing the vortex-shedding from the blunt edge, which is the primary source of TE noise [4]. Another experimental study [5] also demonstrated that the vortex-shedding noise at the TE without serration occurs at a Strouhal number based on TE thickness given by Eq. (1),

$$St_t = \frac{f_v \times t}{U_\infty} \approx 0.1, \tag{1}$$

where $f_v$ is the vortex-shedding peak frequency, $t$ is the thickness of the TE, $U_\infty$ is the free-stream velocity. Howe [2] postulated that the geometry of serrations plays a vital role in noise attenuation and in particular, the serrations with its edge inclined at an angle less than $45^\circ$ were found to significantly reduce the noise levels. Previous experiments have been carried out for an airfoil with continuous serrations at the TE whereas Howe's theoretical model [2] is based on the geometry of an individual serration. Hence, it is necessary to understand the underlying flow and noise physics for an individual serration in an experimental framework to obtain additional insights of its noise reduction capability and also to verify the analytical predictions [2] of noise generated at TE serrations. Therefore, the objective of this paper is to study the effect of individual serration as a noise reduction mechanism through experiments carried out in an Anechoic Wind Tunnel (AWT).

The paper is organised as follows: Section 2 discussed the theoretical background explaining the noise reduction mechanism of an individual TE serration. Next, the experimental set-up of the serrated flat plate model in the AWT is described in Section 3. In Section 4, the Power Spectral Density (PSD) of the radiated noise from the TE of the reference plate for different flow velocities is discussed with a view to illustrate the vortex-shedding TE noise. Furthermore, the 2-D contour plots are presented which shows the reduction in the vortex-shedding TE noise obtained by using a serrated TE as compared to the noise radiated from the reference flat-plate within a particular $St_t$ range. Additionally, source maps obtained using Conventional Beamforming (CB) for different TE serration configurations are compared with that obtained for the reference flat-plate to experimentally demonstrate/validate the noise reduction mechanism of the TE serrations. The paper is concluded in Section 5.

## 2. Theoretical Background

It is shown analytically [2] that the noise is radiated from an edge when the wave number vector $\vec{\mathbf{K}}$ is normal to the edge of the airfoil. In general, the wave number vector $\vec{\mathbf{K}}$, has two components – one normal (along the *z*-direction) and another parallel (along the *x*-direction) to the direction of flow. Figure 2 shows the coordinate system, where *x* is the stream-wise direction, *y* is the span-wise direction and *z* is the vertical direction.

The two components of the wavenumber vectors are denoted by $\vec{\mathbf{K}}_1$ and $\vec{\mathbf{K}}_3$ along the $z$ and $x$ direction, respectively, as indicated in Fig. 2(a). Howe [2] stated that at high-frequencies, corresponding to $0.08 \le St_l \le 0.18$ and low-to-moderate Reynolds number $\mathrm{Re}_c$, the eddy structures convect along the edges due to boundary-layer instability. These eddy structures satisfy the condition $\left|\vec{\mathbf{K}}_1 / \vec{\mathbf{K}}_3\right| \le 1,$ such that the principal acoustic sources are present along the sides of the edges that are inclined at an half-angle $\vartheta$ greater than $45^\circ$ to the free-stream flow. There is no turbulent energy at the wavenumber vector $\vec{\mathbf{K}}$ associated with the direction normal to the edge of the serration, whose half-angle is inclined less than $45^\circ$ to the mean flow. Thus, the serrated TE, which has half-edge angle less than $45^\circ$, results in reduction in the noise levels due to a reduction in the turbulence kinetic energy.

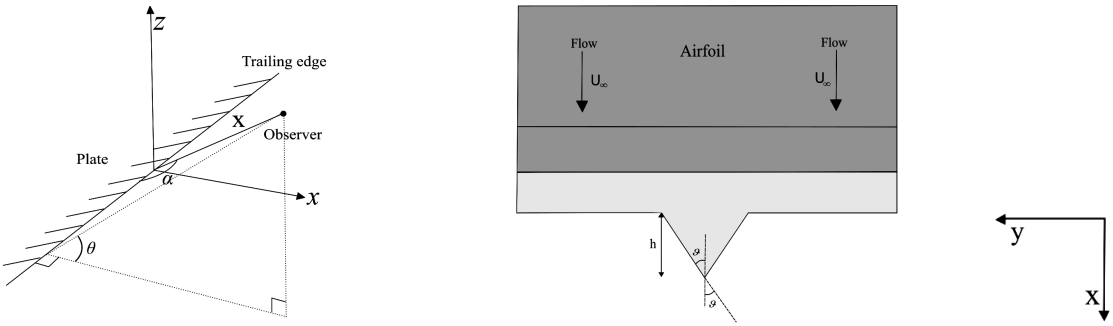


Figure 2. (a) Flat plate co-ordinate system, (b) Single large triangular serration at the TE of the airfoil (Top View) with incidence half-angle $\vartheta$ and the root-to-tip height $h$.

Howe [2] derived the analytical formulation of surface acoustic pressure frequency spectrum in its non-dimensional form shown as follows:

$$\frac{\phi(\omega, x)}{(\rho v_*^2)^2 (b/c)(\delta/|x|)^2} = \left(\frac{C_m}{\pi}\right) \sin^2\left(\frac{\theta}{2}\right) \sin(\alpha) \psi(\omega), |x| \to \infty \tag{2}$$

where $\phi(\omega, x)$ is the surface acoustic pressure frequency spectrum, $\rho$ is the density of fluid, $v_*$ is the friction velocity ($\approx 0.03 U_\infty$), $b$ is the wetted span of the plate, $c_0$ is the sound speed, $\delta$ is the thickness of the boundary-layer, $C_m \approx 0.1153$, $\theta$ and $\alpha$ are the polar and azimuthal observer angles, respectively, as indicated in Fig. 2(a), $\psi(\omega)$ is the non-dimensional edge noise spectrum, $\omega = 2\pi f$ is the angular frequency and $f$ is the frequency in Hz [4]. The non-dimensional edge spectrum $\psi(\omega)$ from the above equation is given as follows:

$$\psi(\omega) = \left(1 + \frac{1}{2}\varepsilon \frac{\partial}{\partial \varepsilon}\right) f\left(\frac{\omega\delta}{U_c}, \frac{h}{\lambda}, \frac{h}{\delta}; \varepsilon\right) \tag{3}$$

where $U_c \approx 0.03 U_\infty$ and $\varepsilon$ = 0.33. Howe [2] showed that as the ratio $h/\lambda$ of root-to-tip to the serration wavelength increases, the components of the wavenumber vector normal to the edge reduces rapidly, thereby attenuating the edge noise. From this result, it was shown that sharper serrations with smaller wavelength and larger root-to-tip distance produces maximum edge noise attenuation. Howe [2] also postulated that noise attenuation is maximum when the height of the serrations is of the order of the turbulent boundary-layer thickness.

## 3. Experimental Set-up

The flat-plate model, presented in Figs. 2(b) and 3, has a TE thickness $t$ = 0.6 mm, LE thickness = 6 mm and the span $b$ = 450 mm. The TE of the airfoil has an unsymmetrical wedge with a $12^\circ$ bevel on the top surface of the airfoil. This particular configuration of airfoil is used for the experiments by Moreau *et al.* [4]. The same airfoil, with different detachable flat plate TE serrations is utilised in the

present work for validation purpose. Five different TE serration configurations and one reference plate (without the TE serration triangle) are used for this experiment as shown in Fig. 4.

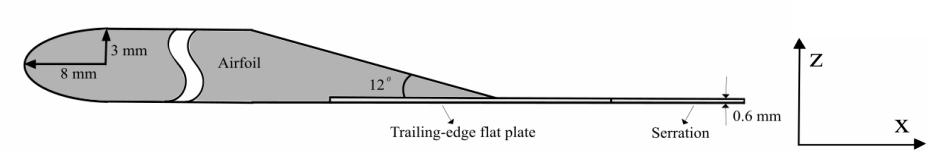


Figure 3. Schematic of the flat plate airfoil with single large TE serration (Side View).

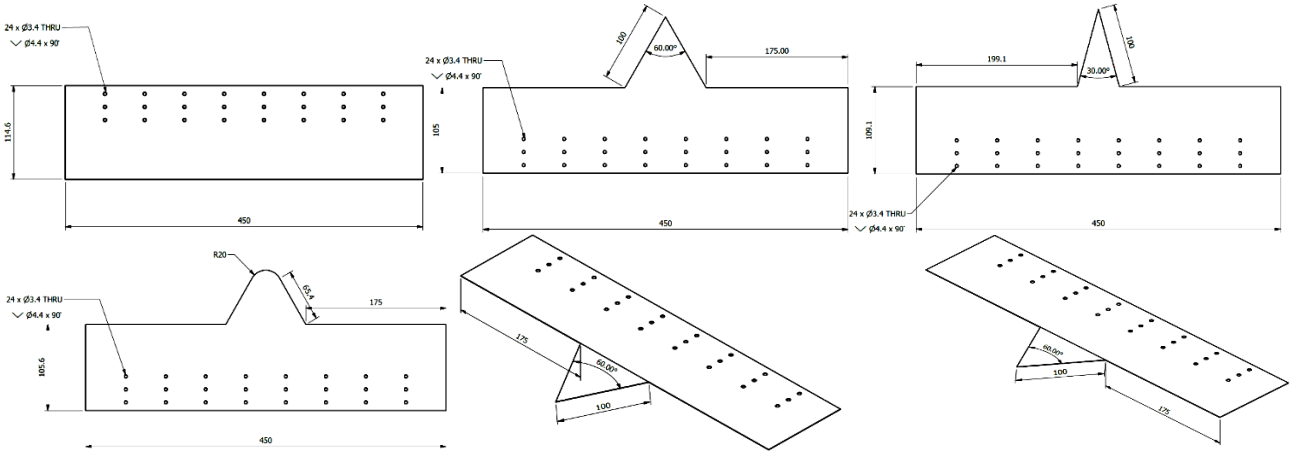

Figure 4. Different TE serration configurations (from top left) – (a) Reference Plate, (b) Serration 1 – Equilateral triangular serration, (c) Serration 2 – Isosceles triangular serration, (d) Serration 3 – Blunt nose serration, (e) Serration 4 – Equilateral serration bent 5$^{o}$ downwards and (f) Serration 5 – Equilateral serration bent 5$^{o}$ upwards.

The noise source radiated from TE is recorded by using a spiral microphone array located along the ceiling of the AWT, i.e., in the plane parallel to the plane of the airfoil at a distance of 530 mm from its TE. Figure 5(a) shows the photograph of a flat-plate model with a narrow TE serration attached to the contraction-outlet of AWT wherein the spiral array of microphones located at the side, (i.e., in the plane perpendicular to the test-model) is shown in the background.

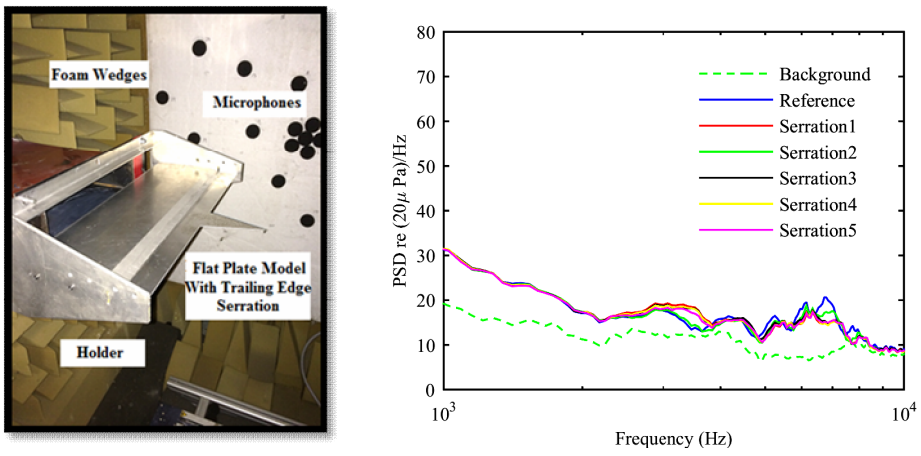


Figure 5. (a) Flat-plate model with a narrow TE serration attached to the contraction-outlet of AWT. (b) PSD plot for different serration configurations at the flow velocity $U_{\infty} = 30\ \mathrm{m \cdot s^{-1}}$.

A replica of the side spiral microphone array is located at the top which is used to record the far-field radiated acoustic pressure. The noise sources are recorded for a sampling time of $T = 40$ s with a sampling frequency $f_S = 2^{16}$ Hz [6]. In order to isolate the microphones from the surrounding wind noise, windsocks are provided on each of the 31 microphones on the top spiral array.

## 4. Results and Discussion

### 4.1 Reference Spectra for Different Flow Velocities

The reference airfoil when tested in the AWT produces vortex-shedding components of noise from the edge [4]. The vortex-shedding TE noise for the reference plate can be obtained by computing its PSD for a range of flow velocities from $U_\infty = 15\ \mathrm{m\cdot s^{-1}}$ to $35\ \mathrm{m\cdot s^{-1}}$. For obtaining the spectral density graphs, the noise data is used from a single microphone from the array which was located directly above the test-model [6]. The PSD is computed using the Welch's averaged modified periodogram method for spectral estimation with a Hanning window and 50% overlap.

It is observed from Fig. 6(a) that for flow velocity $U_\infty = 35\ \mathrm{m\cdot s^{-1}}$, a broad peak is obtained that is centred at a frequency $f$ = 7.7 kHz. This peak decreases in its magnitude and frequency as the flow velocity is reduced as may be observed from Fig. 6(a). This result is in agreement with the previous experimental results [4], where a similar trend was observed in the reference acoustic spectrum.

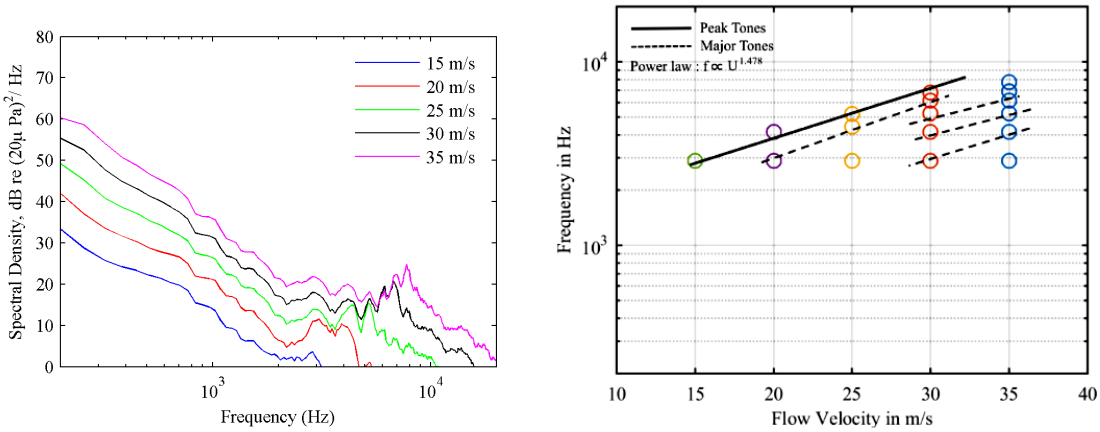


Figure 6. Tonal frequencies scaled with the free-stream velocities for reference plate.

Blake [7] notes that the blunt TE vortex-shedding noise is dependent on the bluntness parameter $t/\delta^*$, where $t$ is TE thickness and $\delta^*$ is the boundary-layer *displacement* thickness. The displacement thickness is calculated from the following approximation [8]

$$\delta = 8\delta^* \tag{4}$$

where $\delta$ can be calculated from the expression for turbulent boundary-layer thickness given by

$$\frac{\delta}{c} = \frac{0.386}{\mathrm{Re}_c^{(1/5)}} \tag{5}$$

where $\mathrm{Re}_c$ is the Reynolds number of the flow based on chord and $c$ is the chord length of the airfoil. The vortex-shedding noise is negligible if the bluntness parameter is less than 0.3 [7]. Table 1 provides information on the bluntness parameter for the experimental reference plate, for a range of flow velocities from $U_\infty = 15\ \mathrm{m\cdot s^{-1}}$ to $35\ \mathrm{m\cdot s^{-1}}$. The values of $t/\delta^*$ obtained from Table 1 indicate that these are greater than 0.3. Hence, the noise at the TE of the airfoil under-consideration is due to the shedding of boundary-layer instability vortices. Table 2 presents the Strouhal number $St_t$ based on the blunt TE thickness given by $St_t = f_v t/U_\infty$ at which the vortex-shedding peaks occur, $f_v$ is the vortex-shedding peak frequency obtained from the reference noise spectral graph for different flow speeds.

Table 1. Airfoil Boundary layer Properties

| Flow velocity, $U_\infty$ | $\delta = \frac{0.386}{\mathrm{Re}^{(1/5)}} * c$ (in m) | $\delta^* = \frac{\delta}{8}$ ($\mathrm{m}^{-1}$) | $\frac{t}{\delta^*}$ |
|---|---|---|---|
| 15 | 0.0064059 | 0.8007 | 0.7493 |
| 20 | 0.0060477 | 0.7559 | 0.7937 |
| 25 | 0.0057838 | 0.7229 | 0.8229 |
| 30 | 0.0055767 | 0.6970 | 0.8607 |
| 35 | 0.0054073 | 0.6759 | 0.8877 |

Table 2. Vortex-shedding peak frequency and the associated Strouhal number $St_t$

| Flow velocity, $U_\infty$ | Vortex-shedding peak frequency $f_v$ (in kHz) | $St_t = f_v t / U_\infty$ |
|---|---|---|
| 15 | 2.88 | 0.11 |
| 20 | 4.16 | 0.12 |
| 25 | 5.184 | 0.12 |
| 30 | 6.784 | 0.13 |
| 35 | 7.744 | 0.13 |

The values of $St_t$ from Table 2 shows that these range between 0.11 and 0.13 and are in a good agreement with the results obtained by Herr *et al.* [5] who showed that the Strouhal number due to blunt TE vortex-shedding noise should be approximately equal to 0.1.

Figure 6(a) indicates that the PSD graph for the reference configuration exhibits peak tones of high amplitude that are produced by airfoils in the high-frequency ranges (above 5 kHz). This peak tone decreases in amplitude and frequency, as the velocity of the airflow is reduced. The inflectional mean velocity profile, caused due to the turbulent boundary-layer instability is responsible for the selection of the tones produced and the corresponding amplification with increase in free-stream velocity [9]. A series of secondary tones accompanies the primary tone. The number and frequency of these secondary tones are also velocity dependent. The amplitude of the peak tones increases linearly with an increase in velocity [10].

From Fig. 6(b), it is observed that the tonal frequencies scale with the free-stream velocity according to power law $\propto U^{1.5}$. Paterson *et al.* [10] found that the spectral analysis of NACA 0012 and NACA 0018 airfoils shows an average increase in the frequencies of the tones according to the power law $\propto U^{1.25}$. Therefore, a small discrepancy is observed with the scaling factor of $n$ = 1.5 which is attributed to the change in geometrical parameters of the airfoil analysed in this work from that considered by Paterson *et al.* [10]. Thus, the experimental results obtained are in good overall agreement with previous work.

### 4.2 Reduction in Noise Levels – Contour plots

The PSD graphs shown in Fig. 5(b) indicates that the reference plate produces an increased noise levels in the high-frequency region while the plate with different serrated configurations produces noise attenuation in this frequency range. Figure 7 shows the 2-D contour plots of the measured reduction in noise levels obtained due to different serration configurations at flow speeds between 15 $\mathrm{m \cdot s^{-1}}$ to 35 $\mathrm{m \cdot s^{-1}}$. The contour plots are obtained by dividing the spectral density of the reference plate by the spectral density of the plate with serrations for different flow velocities which gives the magnitude of reduction in noise levels due to individual serrations. Three distinctive regions of noise levels can be identified from Figs. 7(a) and (b) which are discussed as follows: (1) A region of equal noise level (R1), (2) A region of increased noise levels (R2) and (3) A region of blunt TE vortex-shedding noise attenuation (R3). These regions R1 to R3 are bounded by a constant Strouhal number line based on the TE thickness and are identified as (1) $St_t < 0.04$ as R1, (2) $0.04 \leq St_t \leq 0.08$ as R2 and (3) $0.08 < St_t \leq 0.18$ as R3.

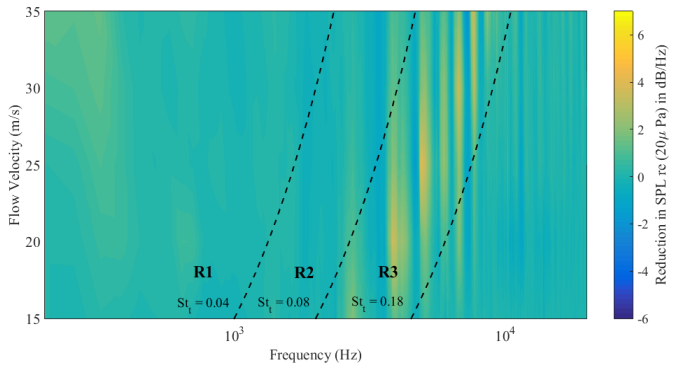


(a)

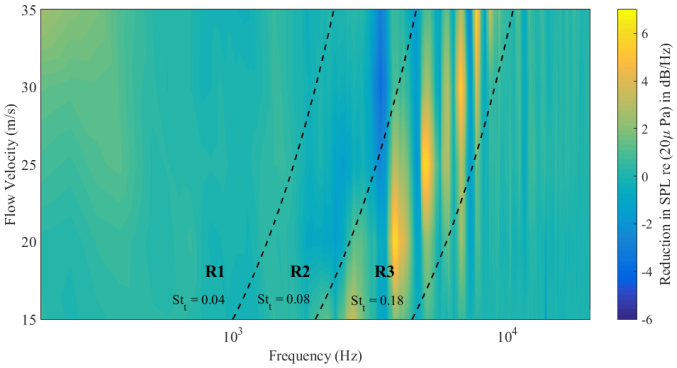


(b)

Figure 7. Noise attenuation due to TE serration from that of the reference plate. The dashed lines represent the lines of constant Strouhal numbers – (a) Serration 2 and (b) Serration 5.

Figures 7(a) and (b) show the 2-D contour plots for Serration 2 and Serration 5, respectively, for the range of free-stream velocities between $U_\infty = 15\ \mathrm{m \cdot s^{-1}}$ to $35\ \mathrm{m \cdot s^{-1}}$. The contour plots for other serration configurations are similar to Serration 5, hence, they are not shown here. It can be observed that the noise reduction is obtained between the Strouhal number ranges from 0.08 up to 0.18 for all mean flow velocities. This shows that the presence of serration reduces the blunt TE vortex-shedding noise, as it is found to occur at $St_t \approx 0.12$ from Section 4.1. It is observed from Fig. 7(b) that Serration 5 produces maximum noise attenuation in the region R3 and minimum increase in noise over the region R2. On the other hand, Fig. 7(a) indicates that unlike Serration 5, the Serration 2 produces minimum noise attenuation. This is because the width of Serration 2 is smaller compared to the plate which renders it ineffective in reducing the TE noise.

### 4.3 Beamforming Plots

The noise sources due to flow over the airfoil are located by implementing the cross-spectral Conventional Beamforming (CB) method. The pressure amplitude measurements obtained from the top microphone array are used for generating the source maps and the colorbar indicates the noise level in dB/Hz. The following symbolic convention are followed in the source maps shown in Figs. 8 to 10 terminologies – (1) the white line at $x = 0$ denotes the contraction-outlet, (2) boundaries of airfoil denoted by a solid white line and (3) the TE of the airfoil is denoted by a dotted white line.

The noise emitted by an arbitrary source will undergo refraction and attenuation while crossing over the shear-layer. Hence, adjustment for shear-layer needs to be incorporated while considering the source radiation properties [12]. Several equations are derived by Amiet [13] for the correction of the shear-layer. The equation used for the correction of shear-layer in this work is taken as $x^* \times M$, where $x^*$ is the half-distance from the centre of the airfoil to the contraction-outlet in the vertical direction, which is equal to 35 mm, $M$ is the Mach number of the mean flow. Table 3 shows the shear-layer corrections (in mm) which denote the distance by which the contraction-outlet is offset towards the

positive *x*-direction (parallel to the free-stream flow direction) in the CB source maps to account for the shear-layer.

Table 3. Shear-layer correction distance for the free-stream velocities from $U_\infty$ = 25 m/s to 35 m/s

| Velocity (in m/s) | Shear-layer correction values for different velocities (in mm) |
|---|---|
| 25 | 2.55 |
| 30 | 3.06 |
| 35 | 3.57 |

The cross-spectral CB results are shown for specific Strouhal numbers, for a free-stream velocity of $U_\infty = 30\ \mathrm{m \cdot s^{-1}}$. The Strouhal numbers are chosen such that they lie within the region of increasing noise R2 given as $0.04 \leq St_t \leq 0.08$ and the region of noise attenuation given as $0.08 < St_t \leq 0.18$ as discussed in section 4.2. The source maps for all the other free-stream velocities and Strouhal numbers follow similar trends, hence, they are not shown here.

Figure 8 shows beamforming source maps from the serrated TE plates and a comparison with the flat-edged reference plate. The noise source locations are indicated by bright yellow spots on the CB source maps. It is observed from Figs. 8(a-f) that TE serrations are ineffective at the Strouhal number $St_t = 0.063$, or equivalently at $f_C = 3.15$ kHz. Similar results were also observed in the mid-frequency range from 2 kHz to 4.9 kHz. The increase in noise in the mid-frequency region is in good agreement with previous experimental results on TE serrations [4].

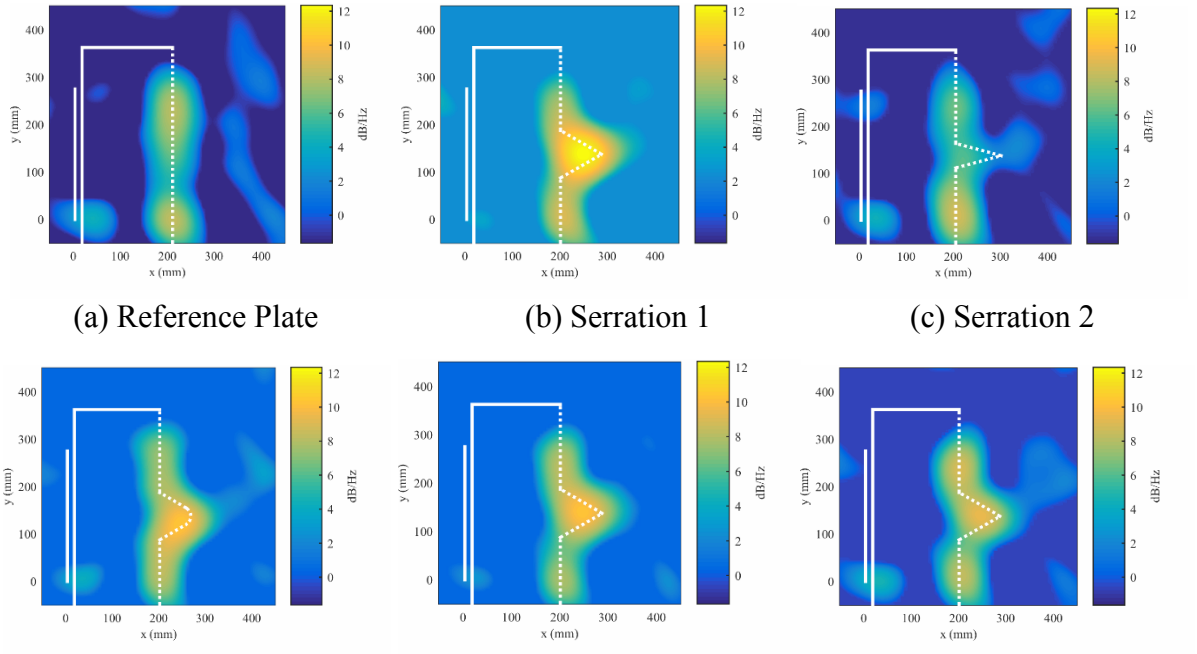


(a) Reference Plate (b) Serration 1 (c) Serration 2

(d) Serration 3 (e) Serration 4 (f) Serration 5

Figure 8. CB source maps for reference and serrated TE plates at $St_t = 0.063$ (which lies within the Strouhal number ranges of $0.04 \leq St_t \leq 0.08$) corresponding to the one-third octave band centre frequency $f_C = 3.15$ kHz for flow velocity $U_\infty = 30\ \mathrm{m \cdot s^{-1}}$.

Figure 9 indicates attenuation in the noise level from the TE of the plate with serrations in comparison to the reference plate at $St_t = 0.1$, or equivalently at $f_C = 5$ kHz. It is noted that the TE noise sources are eliminated along the edges of the serrations and there is a redistribution of noise sources along the straight edges of the TE. In particular, Fig. 9(d) shows that there are certain points along the blunt nose where the effective half-angle $\vartheta$ of the edge to the mean flow is greater than $45^\circ$. Hence, unlike other serrations, noise sources are present along the blunt nose of the serration. It is therefore, concluded that TE serrations act as noise attenuating mechanism for $0.08 < St_t \leq 0.18$ that

corresponds to the high-frequency region, i.e., above 5 kHz. These results are again found to be consistent with previous experimental results on TE serrations [4].

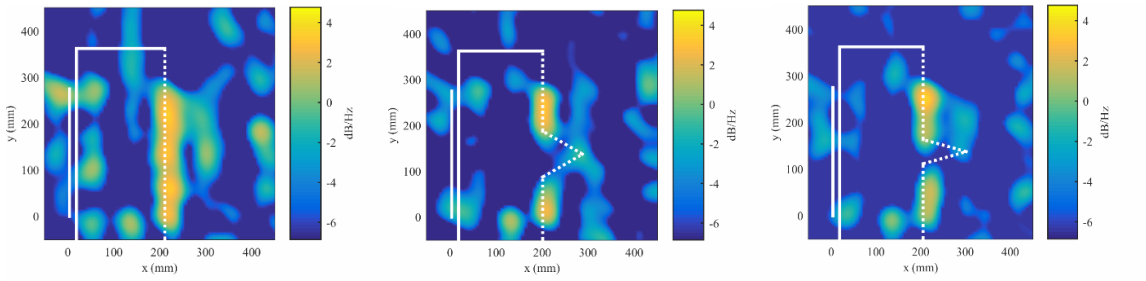


(a) Reference Plate (b) Serration 1 (c) Serration 2

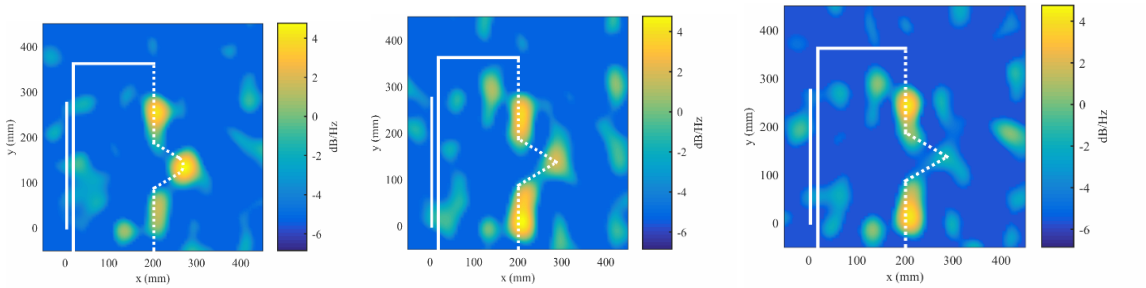


(d) Serration 3 (e) Serration 4 (f) Serration 5

Figure 9. Source maps for reference and serrated TE plates at $St_t = 0.1$ (which lies within the Strouhal number ranges of $0.08 \leq St_t \leq 0.18$) and corresponding to the one-third octave band centre frequency $f_C = 5$ kHz for flow velocity $U_\infty = 30\ \mathrm{m \cdot s^{-1}}$.

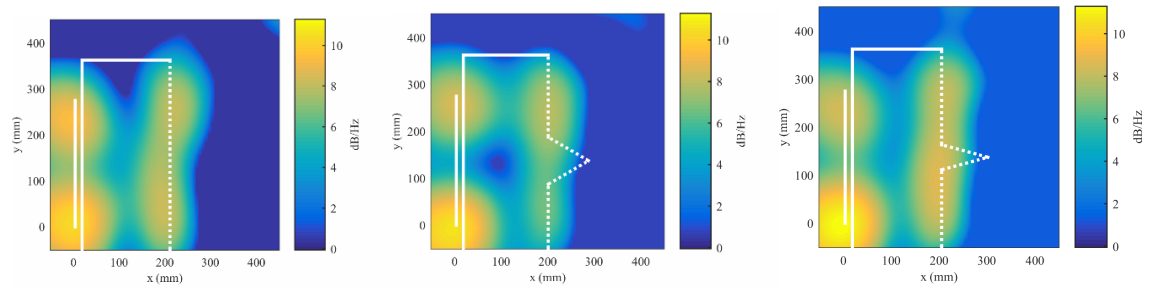


(a) Reference Plate (b) Serration 1 (c) Serration 2

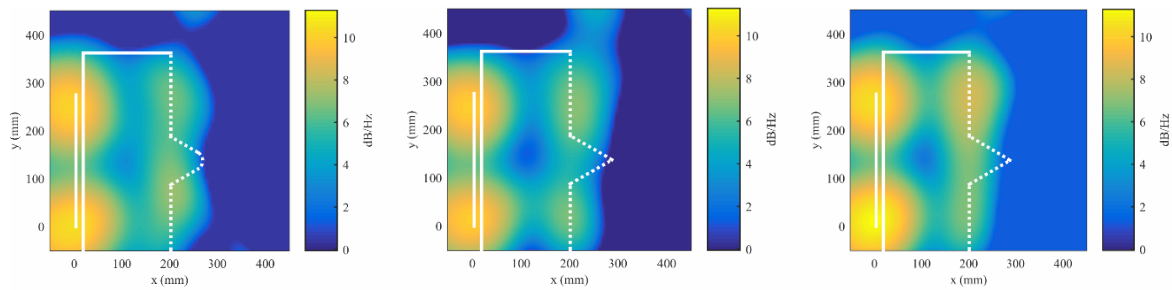


(d) Serration 3 (e) Serration 4 (f) Serration 5

Figure 10. Source maps for reference and serrated TE plates at $St_t = 0.04$ corresponding to the one-third octave band centre frequency $f_C = 2$ kHz for flow velocity $U_\infty = 30\ \mathrm{m \cdot s^{-1}}$.

Figures 10(a-f) shows CB source maps from the serrated TE plates and a comparison with the flat-edged reference plate at $St_t = 0.04$ corresponding to low-frequency $f_C$=2 kHz. It is observed that dominant LE noise sources are present which are centred at the corners of the contraction-outlet instead of spreading along the length of airfoil LE and its occurrence can be explained by phenomenon of shear-layer interaction. The interaction of the shear-layer with the LE generates eddies of length

scales that excites frequencies between 1.75 kHz and 2.5 kHz, thereby causing a dominant LE noise in this frequency range whilst the TE source is significantly weaker.

## 5. Conclusions

This work presents the results of an experimental investigation of the turbulent boundary-layer interaction on various serrated TE edge configurations operating at low-to-moderate Reynolds numbers. The spectral density and the noise attenuation plots indicate that the noise source at the TE of the airfoil under consideration is the blunt TE vortex-shedding noise. These vortex-shedding peak tones follow a ladder structure as suggested by Paterson *et al.* [10]. The CB source maps confirmed the observations by Herr and Dobrzynski [5] that the TE serrations reduce the blunt TE vortex-shedding peak noise which was centred at the Strouhal number $St_t$ range around 0.012. A corresponding noise increase is observed in the mid-frequency range, which is in agreement with the experimental results of Moreau *et al.* [4]. The TE serrations also experimentally validated the Howe's theory [2], in that significant noise attenuation occurs when the half-angle of the edge is less than $45^{\circ}$ to the direction of the mean flow. Furthermore, Howe's theory [2] also states that the height of the TE serrations must be of the order of turbulent boundary-layer thickness for obtaining effective noise attenuation. However, contrary to this theory, the present experimental results showed that the noise attenuation from the TE serrations does not entirely depend on the geometry of serration; rather it depends on the incident angle of the serration edges to the direction of mean flow. Another observation from the CB results is that while TE noise sources dominate at high-frequency [14], the LE noise sources are dominant in the mid-frequency range given by $f_c = 2$ kHz and 2.5 kHz, where $f_C$ is the centre frequency of the corresponding $1/3^{\text{rd}}$ octave band. The increase in the LE noise is attributed to the interaction of the shear-layer (formed at the contraction-outlet) with LE of the test-model.

## References


[1] Doolan, C. J. "A review of airfoil trailing edge noise and prediction", *Acoustics Australia*, **36**, 7-13, (2008).

[2] Howe, M. "Noise produced by sawtooth trailing edge", *Journal of Acoustical Soceity of America*, **90**, 482-487, (1991).

[3] Chase, D. "Noise radiated from an edge in turbulent flow", *AIAA Journal* **13**, 1041-1047, (1975).

[4] Moreau, D. J., Brooks, L. A. and Doolan, C. J. "On the noise reduction mechanism of a flat plate serrated trailing edge at low-to-moderate reynolds number", Colorado Springs, CO, 18th AIAA AIAA/CEAS Aeroacoustic Conference.

[5] Herr, M. and Dobrzynski, W. "Experimental investigaiton in low-noise trailing edge design," *AIAA Journal*, **43**, 1167-1175, (2005).

[6] Moreau, D. J., Prime. Z., Porteous. R., Doolan. C. J. and Valeau. V. "Flow induced noise of a wall-mounted finite airfoils for low-to-moderate reynolds number", *Journal of Sound and Vibration*, **333**, 6924-6941, (2014).

[7] Blake, W. Mechanics of flow induced sound and vibration, Vol II. Academic Press, London, 1986.

[8] Cebeci, T. and Bradshaw, P. *Momentum transfer in boundary layer*, Hemisphere Publications, Washington D.C, 1977.

[9] Moreau, D. J., Brooks, L. A. and Doolan, C. J., "Broadband trailing edge noise from a sharp-edged strut", *Journal of the Acoustical Soceity of America*, **129**, 2820-2829, (2011).

[10] Paterson, R., Vogt, P. and Fin, M. "Vortex noise of isolated airfoils", *Journal of Aircraft*, **10**, 296-302, (1973).

[11] Porteous, R., Prime. Z., Valeau. V., Doolan. C. J. and Moreau. D. J. "Three-dimensional beamforming of aeroacoustic sources", Melbourne, Internoise, 2014.

[12] Porteous, R., Doolan, C. J. and Moreau, D. J. "Directivity pattern of flow induced noise from wall-mounted finite length circular cylinder", Proceedings of Acoustics, Victor Harbour, 2013.

[13] Amiet, R. "Correction of open jet wind tunnel measurements for shear layer refraction", Hampton, VA, AIAA 2nd Acoustics Conference, 1975.

[14] Mimani, A., Moreau, D. J. and Doolan, C. J. "Experimental application of aeroacoustic time-reversal", Proceedings of the 21st AIAA/CEAS Aeroacoustics Conference, Dallas, 2015.